Pis'ma v ZhETF, vol. 98, iss. 9, pp. 620 – 625 

# Breathing charge density waves in intrinsic Josephson junctions

*Yu. M. Shukrinov*[+1)], *H. Abdelhafiz*[+*]

[+]*Bogoliubov Laboratory of Theoretical Physics, Joint Institute for Nuclear Research, 141980 Dubna, Russia*

[*]*Nile University, Smart Village, 12677 Giza, Egypt*

Submitted 23 August 2013
Resubmitted 3 October 2013

We demonstrate the creation of a charge density wave (CDW) along a stack of coupled Josephson junctions (JJs) in layered superconductors. Electric charge in each superconducting layer oscillates around some average value, forming a breathing CDW. We show the transformation of a longitudinal plasma wave to CDW in the state corresponding to the outermost branch. Transition between different types of CDW's related to the inner branches of $IV$-characteristic is demonstrated. The effect of the external electromagnetic radiation on the states corresponding to the inner branches differs crucially from the case of the single JJ. The Shapiro steps in the $IV$-characteristics of the junctions in the stack do not correspond directly to the frequency of radiation $\omega$. The system of JJs behaves like a single whole system: the Shapiro steps or their harmonics in the total $IV$-characteristics appear at voltage $\sum V_l = N_R \frac{m}{n}\omega$, where $V_l$ is the voltage in $l$-th junction, $N_R$ is the number of JJs in the rotating state, and $m$ and $n$ are integer numbers.

DOI: 10.7868/S0370274X13210078

Charge density waves (CDW) are well known in different low dimensional systems, as well as cuprate superconductors [1–5]. Recently, the CDWs were discovered in $YBa_2Cu_3O_{6+x}$ [6, 7]. It was stressed in Ref. [8] that "this discovery places charge orders center stage with superconductivity, suggesting that they are intertwined rather than competing". In contrast to these classical CDWs, where the origin of CDW is related to the peculiarities of the Fermi surface [1], another type of CDW related to the non-equilibrium nature of the AC (alternating current) Josephson effect in HTSC (high temperature superconductor) is possible. Machida et al. [9] demonstrated the instability of longitudinal plasma waves in the states corresponding to the inner branches and showed that there is a static CDW along the $c$-axis. They suggested that the branching of $IV$-characteristics is a result of transitions between different spatial CDW modes.

In this Letter, we discuss the nature of different CDW spatial modes realized due to the coupling between intrinsic Josephson junctions (JJ) in HTSC. We suggest a mechanism of formation of CDWs as states with different numbers of Josephson junctions in the rotating (R) and oscillating (O) states [10]. Two different types of breathing CDW related to the outermost branch and inner branches of the $IV$-characteristics are demonstrated. We stress a different origin for CDWs realized in the states corresponding to the inner branches of the $IV$-characteristics. The influence of the external electromagnetic radiation on the states corresponding to the inner branches cardinally differs from that for the outermost branch or for single JJ. We demonstrate that the Shapiro step in the $IV$-characteristics of each junction of the stack does not correspond to the radiation frequency directly. System of coupled JJs reacts as a single one.

To investigate the CDW in HTSC we use the one-dimensional capacitively coupled Josephson junction model with diffusion current (CCJJ+DC model) [11, 12] with the gauge-invariant phase differences $\varphi_l(t)$ between S-layers $l$ and $l+1$ described by the system of equations:

$$\begin{cases} \dfrac{\partial \varphi_l}{\partial t} = V_l - \alpha(V_{l+1} + V_{l-1} - 2V_l), \\ \dfrac{\partial V_l}{\partial t} = I - \sin\varphi_l - \beta\dfrac{\partial \varphi_l}{\partial t} + A\sin\omega t + I_l^{\rm noise}, \end{cases} \tag{1}$$

where $t$ is the dimensionless time normalized to the inverse plasma frequency $\omega_p^{-1}$ ( $\omega_p = \sqrt{2eI_c/\hbar C}$, $C$ is the capacitance of the junctions, $\beta = 1/\sqrt{\beta_c}$, $\beta_c$ is the McCumber parameter), $\alpha$ gives the coupling between junctions [13], $\omega$ and $A$ are the frequency and amplitude of the external electromagnetic radiation, respectively.

To find the $IV$-characteristics of the stack of the intrinsic JJs, we solve this system of nonlinear differential equations (1) using the fourth order Runge–Kutta method. As a result, we find the temporal dependence of the voltages in each junction at a fixed value of bias cur-

[1)]e-mail: shukrinv@theor.jinr.ru

rent $I$. Then the current value is increased or decreased by a small amount of $\delta I$ (bias current step) to calculate the voltages in all junctions at the next point of the $IV$-characteristics. So actually time dependence of voltage in each junction or charge in each layer consists of intervals at each fixed current value. We use the distribution of phases and voltages achieved at the previous point of the $IV$-characteristics as the initial distribution for the current point. The average of the voltage $\bar{V}_l$ is given by $\bar{V}_l = \frac{1}{T_f - T_i} \int_{T_i}^{T_f} V_l dt$ where $T_i$ and $T_f$ determine the interval for the temporal averaging. Total voltage in the stack is determined as a sum of these voltages. In our simulations we measure the voltage in units of $V_0 = \hbar\omega_p/(2e)$, the frequency in units of $\omega_p$, and the bias current $I$ in units of $I_c$. Time dependence of the electric charge in the superconducting layers is investigated by Maxwell equation $\mathrm{div}(\varepsilon\varepsilon_0 \mathbf{E}) = Q$.

The charge density $Q_l$ (in the following text referred to as charge) in the S-layer $l$ is proportional to the difference between the voltages $V_l$ and $V_{l+1}$ in the neighbor insulating layers $Q_l = Q_0\alpha(V_{l+1} - V_l)$, where $Q_0 = \varepsilon\varepsilon_0 V_0/r_D^2$. Numerical calculations have been done for a stack with 10 Josephson junctions, the coupling parameter $\alpha = 1$, dissipation parameter $\beta = 0.2$ and periodic boundary conditions. Coupling between junctions leads to the creation of the rotating (the time average of $\partial\varphi(l)/\partial t$ is constant and that of $\sin[\varphi(l)]$ is zero) and oscillating (the time average of $\partial\varphi(l)/\partial t$ is zero and that of $\sin[\varphi(l)]$ is constant) states [10]. The O-state is one of the new elements which appear in IJJ in comparing with one JJ. The O-state can be realized if number of junctions in the stack is more than two. In all calculations a noise with the amplitude $I_{\mathrm{noise}} = 10^{-8}$ generated by a random number generator was added to the bias current. The amplitude of noise was normalized to the critical current $I_c$. Details of the model and simulation procedure can be found in Ref. [14].

Let us first consider results related to the transition from the outermost branch (all junctions in R-state) to inner branch (some junctions in O-state). Such a transition happens in the resonance region, where a longitudinal plasma wave (LPW) with a definite wave number is created. In the parametric resonance region [15] we observe the charge oscillations corresponding to the $\pi$-mode of the LPW (see inset in Fig. 1a).

In Fig. 1a we show the $Q(t)$ dependence together with the $IV$ characteristics (thin curve with diamond symbols) near transition from the outermost branch to an inner branch with three JJs in the R-state (branch number *3* in Fig. 1c). The $Q(t)$ dependence shown, is characterized by exponential increase of the charge in the S-layers in the parametric resonance region (char-

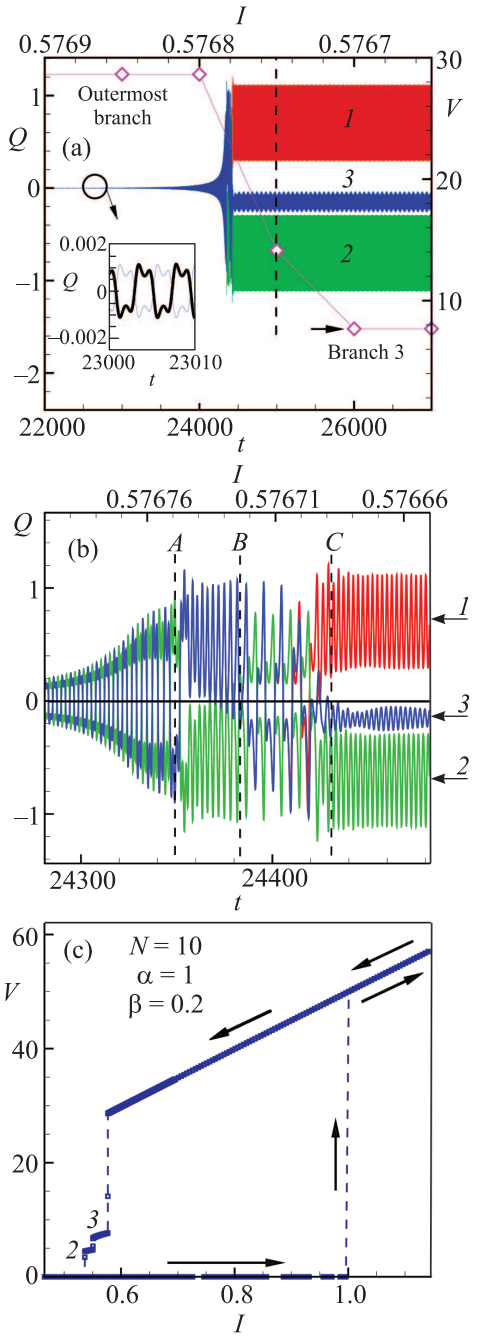


Fig. 1. (Color online) (a) – Charge in the S-layers as a function of time together with the $IV$-characteristics (curve with the diamond symbols related to the right and upper axes) near transition from the outermost branch to inner branch 3. The dashed line passing through the current symbol stresses that the system is in the CDW-state. The inset shows the LPW oscillations ($\pi$-mode). (b) – The enlarged part of the $Q(t)$ dependence demonstrating the transition LPW $\rightarrow$ CDW. (c) – One-loop $IV$-characteristics for the same stack. The arrows show the directions of bias current changes throughout the simulation

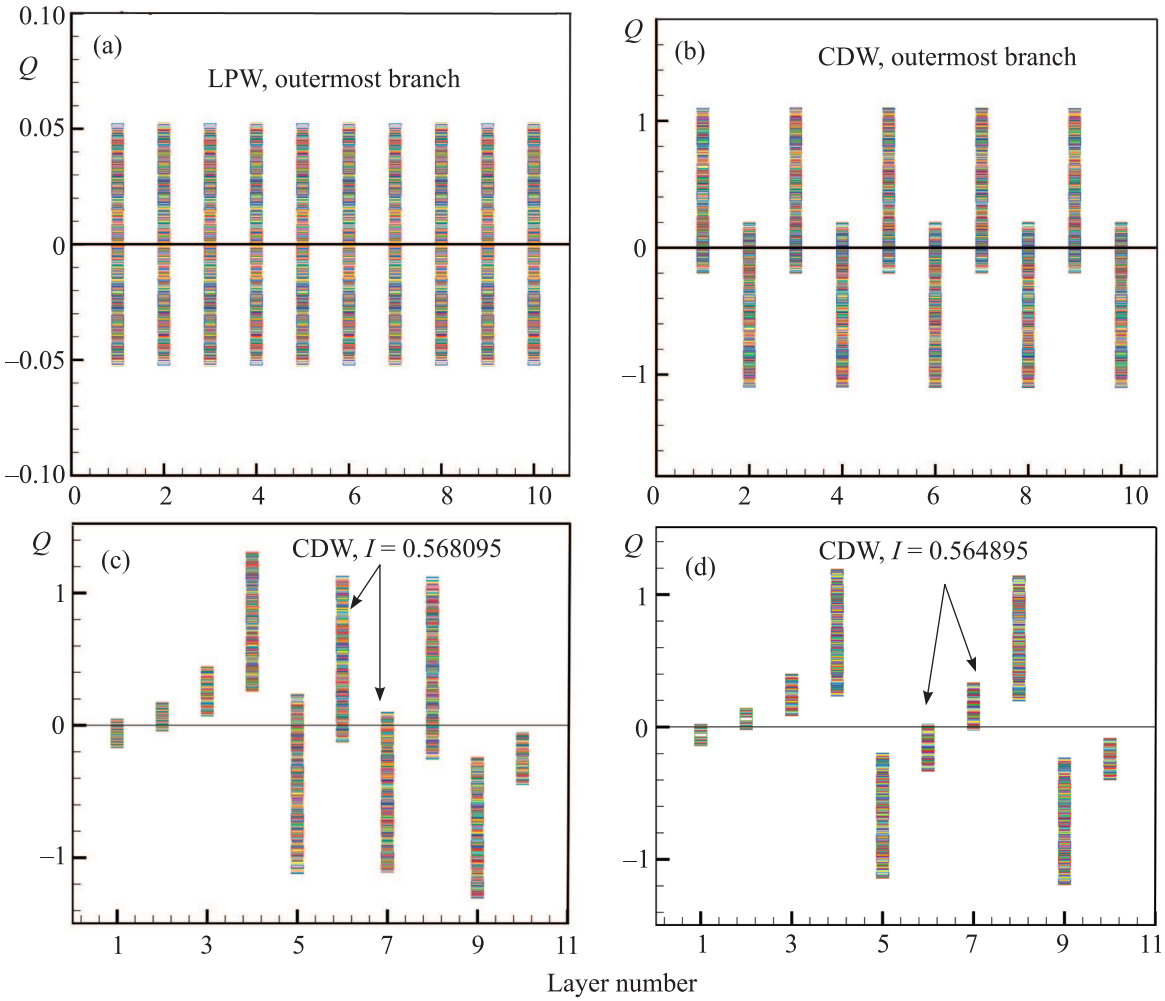


Fig. 2. (Color online) (a) – Charge variation intervals in all layers of the stack during time domain before point $A$ in Fig. 1b. (b) – The same in the $A-B$ region. (c) – CDW corresponding to the inner branch 3 at $I/I_c = 0.568095$ (before transition to branch 2). (d) – CDW after transition to branch 2 at $I/I_c = 0.564895$. Arrows stress the change of the charge variation intervals in S-layers 6 and 7

acter of charge oscillations in two first layers is shown in the inset to Fig. 1a), some transition region, and by oscillations of different amplitude around different average values in each superconducting layer of the stack. To simplify the picture, we show the charge oscillations in three layers only. So, the branch 3 corresponds to the state with a CDW: the electric charge in each superconducting layer oscillates around some average value forming a breathing CDW along the stack. To stress this fact we plot in Fig. 1a the dashed line passing through the current symbol corresponding to the current value $I = 0.57675$. We note that the transition from one branch to the other is a result of the phase dynamics of the system, and it is not related directly to the change of the bias current value. The dynamical transition from the outermost branch to branch 3 happens in one time domain, i.e. at one step in bias current between $I = 0.57680$ and $0.57675$. Intermediate values of voltage between two branches correspond practically to the formed CDW, and their values depend on the time interval which the system spent in the formed state.

Figure 1b illustrates the enlarged part of the $Q(t)$ dependence around the transition from the LPW to the CDW state corresponding to the outermost branch (all JJs in R-state). The CDW forms in the current interval with initial current value related to the outermost branch. We can distinguish four different regions here. Before point $A$ the system is in the state with LPW. Then, in region $A-B$ we can see the breathing CDW, when the charge in odd layers breaths around positive average value, while the charge in the even layers breaths around negative average value. The time interval the system spend in this state is short enough. In the region $B-C$ the system is in CDW state also, but

the averaged values of charge in odd and even layers are decreased compared with $A-B$ region. After point $C$ the system goes to the state with CDW related to the inner branch. Analysis shows that it is a branch *3* with 3 JJs in the rotating state.

Let us now consider the charge oscillations in S-layers before the point $A$ (see Fig. 1b) again. If we plot the values of charge in each layer in time, we get the distribution of charge along the stack presented in Fig. 2a. The charge distribution in the $A-B$ region is shown in Fig. 2b. *We see clearly the LPW in the first case and the breathing CDW in the second one.*

The intervals of charge oscillations in different layers in the CDW state, corresponding to the inner branch 3 (see Fig. 1c) are shown in Fig. 2c. We see that in the four S-layers $(1, 2, 3, 10)$ the value of charge is much smaller compared with other layers. So, we observe another type of CDW in compare with Fig. 1b.

Now we consider the transformation from one CDW to another, which is related to transitions between inner branches of the $IV$-characteristics. Fig. 1c shows the $IV$-characteristics with the following transitions: from outermost branch $OB \to$ branch 3 $\to$ branch 2 $\to$ zero voltage state. The corresponding CDWs in the branches 2 and 3 are shown in the Fig. 2c and d. Transition $3 \to 2$ corresponds to the transformation of one JJ from the R-state to the O-state. Comparing the CDWs shown in (c) and (d), we see that this additional transition has occurred between layers 6 and 7, as shown by the arrows in the insets.

To explain the structure of CDW, realized in the states corresponded to the inner branches, we use the idea that an inner branch corresponds to the state with JJs in R- and O-states [10]. First we discuss what we would obtain if one JJ of the stack is in the O-state. Let it be JJ between S-layers 5 and 6 as shown in Fig. 3a, so voltage $V_5$ is close to zero. We reflect the qualitative picture only. Because the charge in the 5-th S-layer is proportional to the voltage difference between neighboring JJs, i.e. to $V_5 - V_4$, its value is negative. By the same reasoning the charge in layer 6 is positive. As a result, we expect the CDW with the shape, shown in Fig. 3a by pluses and minuses. It counts the charge value relative to the dashed line. The two cases with two JJs in the O-state, neighbor and separated with corresponding CDWs are presented in Figs. 3b and c, respectively.

For example, using this type of modeling, we can easily explain the results of Fig. 2c and reproduce the created CDW. Because the charge's sign in the layers 4 and 5, 6 and 7, and 8 and 9 is changing from plus to minus, the corresponding JJs (4, 6, and 8) are in the rotating state as shown in the upper part of Fig. 3d.

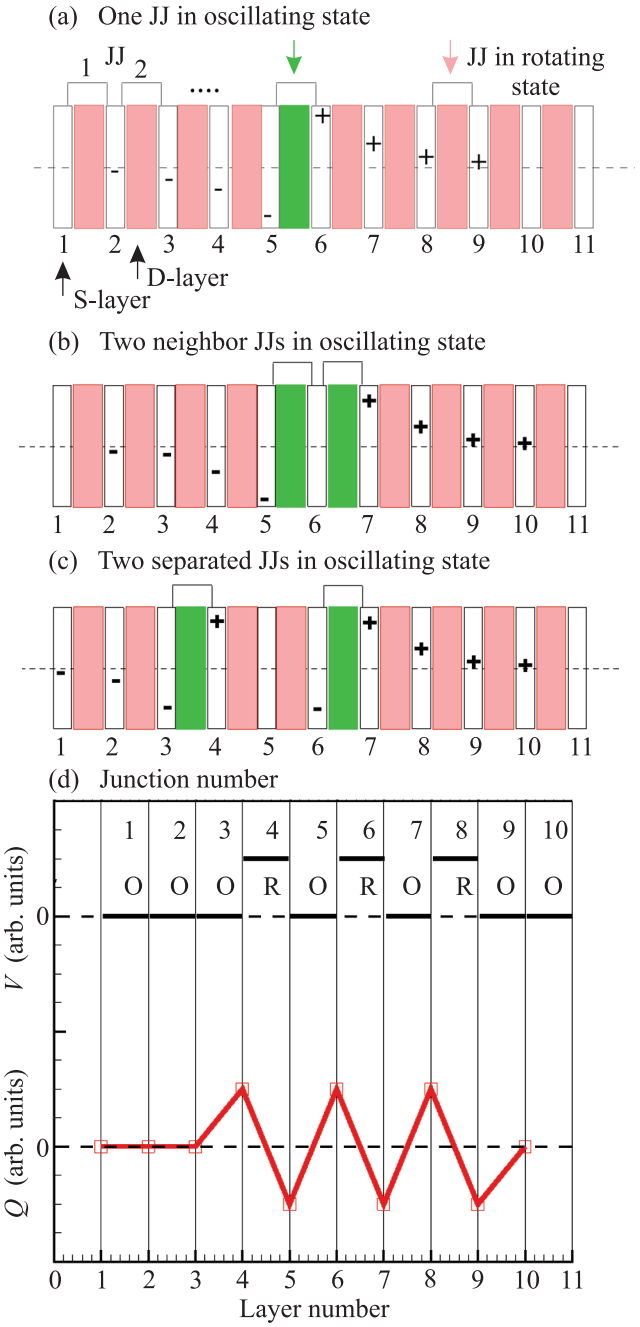


Fig. 3. (Color online) Modeling of charge distribution along the stack: (a) – one oscillating JJ; (b) – two neighbor oscillating JJs; (c) – two separated oscillating JJs. (d) – Schematic explanation of the CDW origin: (up) distribution of voltage among JJs; (down) distribution of charge among the S-layers

Taking into account that charge is proportional to the difference in voltage between neighboring junctions, we find that the CDW has the structure shown in Fig. 3d, in agreement with the results in Fig. 2c.

Let us now discuss the effect of the external radiation on CDW corresponding to the inner branch. Figure 4a

shows the $IV$-characteristics of all JJs in the stack with 10 JJs under radiation with the frequency $\omega = 1.5$ and amplitude $A = 0.5$. The $IV$-characteristics are coincide before transition to inner branch (point $B$) and we see here the Shapiro step at $V = 3$, which corresponds to the second harmonic $2\omega$. Then we observe transitions to the inner branch and between inner branches. The $IV$-characteristic of the total stack (Fig. 4b manifests four inner branches, two of them are very small). Their analysis shows that the lowest one corresponds to the state ORROOORROO with four junctions in the rotating state. The $IV$-characteristic of the total stack demonstrates the step at $V = 9$ corresponding to the $3\omega/2$ Shapiro harmonic, which is in agreement with $V = N_R \frac{m}{n}\omega$ at $N_R = 4$, $m = 3$, and $n = 2$.

If all JJs in the stack were independent and reacted in the same way on the external radiation, we would observe the steps at $V = 2.25$ in the $IV$-characteristics of all these four rotating JJs . However, as we see in the insets to Fig. 4a, the Shapiro steps appear at absolutely different values. We stress that Fig. 4a demonstrates the $IV$-characteristics of all JJs in the stack. We see that some parts of these characteristics for different junctions are coincide. The distribution of the Shapiro step's voltage is shown in Fig. 4c. Four JJs show steps at $V = 1.4318$ (they are in R-state), the other four at $V = 0.6138$ (O-state) and two JJs show steps at $V = 0.4093$ (O-state). These values are shown by triangles. The sum of these voltages in all JJs of the stack is equal to $V = 9$. *This fact indicates that the system of Josephson junctions behaves like a single whole system.*

To stress this phenomenon, we show additionally in Fig. 4c the distribution of junction's voltage at the same frequency but with a smaller amplitude $A = 0.05$. In this case, the branch with four rotating junctions is also realized in the total $IV$-characteristic of the stack but with another distribution OORRORROOO of rotating and oscillation junctions. This branch also demonstrates the Shapiro step at $V = 9$. Squares and diamonds show the distribution of voltage along the stack above the Shapiro step and at the Shapiro step, respectively ($IV$-characteristic is not shown here). In this case we observe the same feature: *the sum of the voltages in all JJs is equal to* $V = 9$.

In the case when all JJs of the stack are in the rotating state (outermost branch), the Shapiro steps are realized at the same value of voltage in each $IV$-characteristic of the corresponding JJ, i.e., in a usual way. We see in Fig. 4a that all $IV$-curves of JJs in the stack demonstrate the Shapiro steps at the same value of voltage $V = 3$. So, we stress once again: when one or some JJs of the stack turn into the O-state, we observe

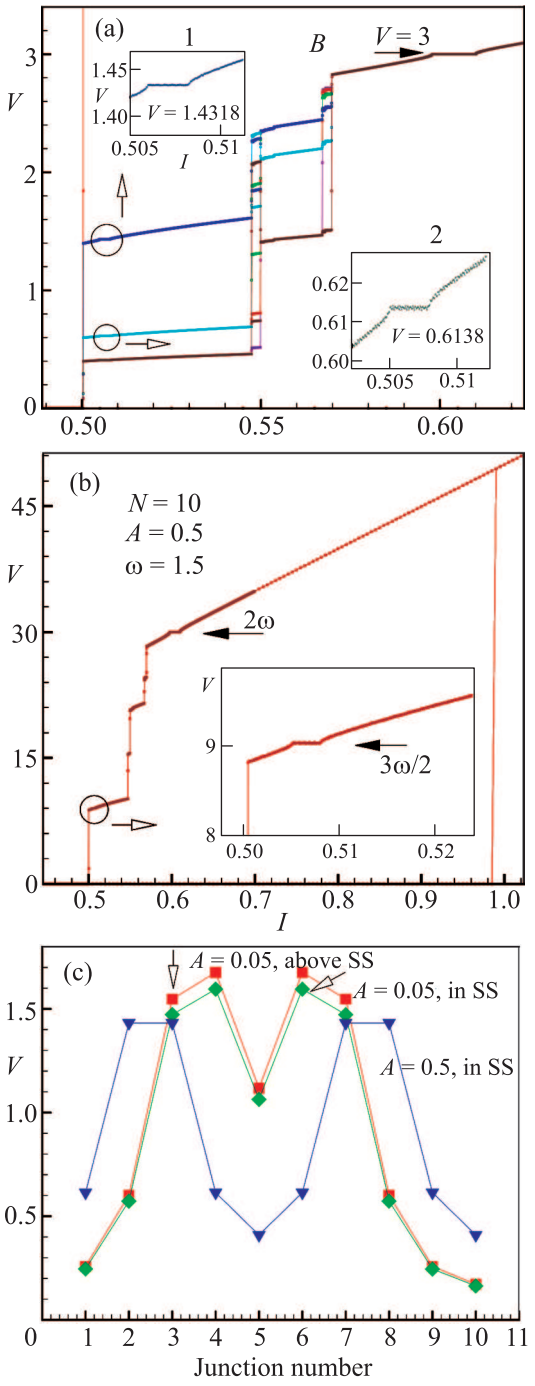


Fig. 4. (Color online) (a) – Parts of $IV$-characteristics of all JJs in the stack in the branching region. Insets enlarges the parts with the Shapiro steps in two characteristics of different JJs. (b) – $IV$-characteristics of the total stack. Inset demonstrates the Shapiro step in the inner branch, when all JJs in R-state. (c) – Distribution of voltage along the stack at $A = 0.5$ at the Shapiro step (triangle) and at $A = 0.05$ above the Shapiro step (square) and at the Shapiro step (diamond)

the system of the Shapiro steps at different voltages. The radiation frequency "manifests itself directly" in the $IV$-

characteristics of the whole stack only, i.e., the system of coupled Josephson junctions behaves like an entire one.

Let us discuss shortly the possibility of the experimental testing of the obtained results. The charge $Q_l$ in the S-layer $l$ is proportional to the difference between the voltages $V_l$ and $V_{l+1}$ in the neighbor insulating layers $Q_l = Q_0\alpha(V_{l+1} - V_l)$, where $Q_0 = \varepsilon\varepsilon_0 V_0/r_D^2$. For $r_D = 3 \cdot 10^{-10}$ m, $\varepsilon = 25$, $\omega_p = 10^{12}\,\mathrm{s}^{-1}$ we get $V_0 = 3 \cdot 10^{-4}$ V and $Q_0 = 8 \cdot 10^5\,\mathrm{C/m}^3$. So at $Q = Q_0$ for a superconducting layer with the area $S = 1\,\mu\mathrm{m}^2$ and thickness $d = 3 \cdot 10^{-10}$ m the charge value is about $2.4 \cdot 10^{-16}$ C. This value of charge is not high but it creates novel interesting physics and can be measured experimentally.

To summarize, we note that the use of intrinsic JJs as elements for superconductive electronics requires the knowledge of mechanisms of $IV$-characteristics branching and switching between states with different numbers of oscillating and rotating Josephson junctions. Different inner branches of $IV$-characteristics of the stack with $N$ JJs reflect the states with different combination of R- and O-states [10, 13, 14, 16]. Each of these combinations is associated with particular CDW. We demonstrated that in the system of coupled JJs within the hysteretic region, a transition from outermost to inner branch is caused by the transformation of a LPW to a breathing CDW. At such transition we also found a formation of an evanescent CDW or LPW from the states attributed to the outermost branch (with all junctions in the rotating state). The breathing CDW is a characteristic of the inner branch and it is specified by the number of JJs in the rotating and oscillating states, as well as their positions in the stack. Transitions between inner branches are caused by the transformation of one type of CDW to another one. The interesting new features of the coupled Josephson junctions appear under external electromagnetic radiation. The effect of this system in the CDW state is completely different from the reaction of single JJ on the external radiation. It causes the appearance of the set of the Shapiro steps in the $IV$-characteristics of JJs of the stack related to the voltage distribution among JJs. However, usual harmonics and subharmonics of radiation frequency are observed in the $IV$-characteristics of the total stack. I.e., we stress that the stack in CDW states reacts on a microwave radiation as a whole, showing the right Shapiro steps values in total voltage. This new finding should stimulate additional investigations of coupled JJs under electromagnetic radiation both theoretically and experimentally.

We thank I.R. Rahmonov, M. Gaafar, A.E. Botha, M.R. Kolahchi, P. Seidel for fruitful discussions. We acknowledge the support from JINR-EGYPT collaboration.

1. G. Gruner, *Density Waves in Solids*, Addison-Wesley Pub. Co., Advanced Book Program, 1994.
2. D. Moncton, J. Axe, and F. DiSalvo, Phys. Rev. B **16**, 801 (1977).
3. M. Fujita, H. Goka, K. Yamada, and J. Tranquada, Phys. Rev. B **70**, 104517 (2004).
4. S. A. Kivelson, I. P. Bindloss, V. Oganesyan, and J. M. Tranquada, Rev. Mod. Phys. **75**, 1201 (2003).
5. M. Vojta, Advances in Physics **58**, 699 (2009).
6. J. Chang, E. Blackburn, A. T. Holmes, and N. B. Christensen, Nature Phys. **8**, 871 (2012).
7. G. Ghiringhelli, M. Le Tacon, M. Minola, and S. Blanco-Canosa, Science **337**, 821 (2012).
8. E. Fradkin and S. A. Kivelson, Nature Phys. **8**, 864 (2012).
9. M. Machida, T. Koyama, A. Tanaka and M. Tachiki, Physica **C 330**, 85 (2000).
10. H. Matsumoto, S. Sakamoto, F. Wajima, and T. Koyama, Phys. Rev. B **60**, 3666 (1999).
11. Yu. M. Shukrinov, F. Mahfouzi, and P. Seidel, Physica C **449**, 62 (2006).
12. Yu. M. Shukrinov and I. R. Rahmonov, JETP **115**, 289 (2012).
13. T. Koyama and M. Tachiki, Phys. Rev. B **54**, 16183 (1996).
14. Yu. M. Shukrinov, F. Mahfouzi, and N. F. Pedersen, Phys. Rev. B **75**, 104508 (2007).
15. Yu. M. Shukrinov and F. Mahfouzi, Phys. Rev. Lett. B **98**, 157001 (2007).
16. Yu. M. Shukrinov and F. Mahfouzi, Physica C **434**, 6 (2006).